

# Poles and zeros of electromagnetic quantities in photonic systems

Felix Binkowski,<sup>1</sup> Fridtjof Betz,<sup>1</sup> Rémi Colom,<sup>2</sup> Patrice Genevet,<sup>2,3</sup> and Sven Burger<sup>1,4</sup>

<sup>1</sup>Zuse Institute Berlin, 14195 Berlin, Germany

<sup>2</sup>Université Côte d'Azur, CNRS, CRHEA, 06560 Valbonne, France

<sup>3</sup>Physics Department, Colorado School of Mines, Golden, Colorado 80401, USA

<sup>4</sup>JCMwave GmbH, 14050 Berlin, Germany

We present an approach to investigate poles and zeros in resonant photonic systems. The theory is based on contour integration of electromagnetic quantities and allows to compute the zeros, to extract their sensitivities with respect to geometrical or other parameters, and to perform modal expansions in the complex frequency plane. The approach is demonstrated using an example from the field of nanophotonics, an illuminated metasurface, where the emergence of reflection zeros due to the underlying resonance poles is explored.

In the field of photonics, light-matter interactions can be tuned by exploiting resonance phenomena. Examples include tailoring quantum entanglement with atoms and photons in cavities [1], probing single molecules with ultrahigh sensitivity [2], and realizing efficient single-photon sources [3]. While electromagnetic observables are measured at real-valued excitation frequencies, the concept of resonances intrinsically considers the complex frequency plane [4, 5]. Resonance frequencies are complex-valued as the systems exhibit losses, e.g., due to interaction with the environment. Excitation of the systems close to the resonance frequencies, which are the poles of the electromagnetic field, leads to highly increased field values. An important figure of merit is the quality factor of a resonance, which is defined as the scaled ratio of real and imaginary part of the corresponding pole, and which can represent the relation between stored and dissipated electromagnetic field energy of the resonance [6]. Resonances can also serve as a basis for the expansion of electromagnetic quantities. Although most nanophotonic systems support many resonances, often only a few resonances are sufficient to determine the optical response in the real-valued frequency range of interest [7, 8].

The design of photonic components can be greatly simplified by determining the complex frequency response of the photonic systems. Controlling the relative locations of complex-valued poles and zeros of the scattering matrix or of the transmission or reflection coefficients can serve as a basis to tailor the corresponding optical response. This kind of approach has long been used to design electronic systems [9]. For example, all pass filters, i.e., systems whose response amplitude remains constant when the excitation frequency is varied, have poles and zeros which are complex conjugated [10]. Other examples are minimum-phase systems, where the zeros have to be restricted to the lower part of the complex plane [11, 12]. In photonics, recently, it has been shown that a  $2\pi$ -phase gradient of the reflection or transmission output channel of a metasurface can be realized when a pair of pole and zero is separated by the real axis in the complex frequency plane [13]. Moreover, the zeros can have ar-

bitrarily small imaginary parts, i.e., the analysis of the locations of the zeros is extremely relevant to design the response of the photonic systems at real frequencies. Total absorption of light or perfect coherent absorption occurs when zeros of the scattering matrix are on the real axis [14–16]. Reflection zeros are also exploited for phase-sensitive detection with nanophotonic cavities in biosensing applications [17, 18].

While in many electronic systems the determination of poles and zeros of the transfer matrix may be done analytically, this is often not possible for photonic structures, such as metasurfaces. To compute reflection and transmission zeros of scattering matrices of specific systems, it has been proposed to solve Maxwell's equations as an eigenproblem with appropriately modified boundary conditions [19–21].

In this work, we present an approach for the study of poles and zeros in arbitrary photonic systems. The theory is based on contour integration of electromagnetic quantities which allows to extract also sensitivities of the poles and zeros, i.e., their evolution in the complex frequency plane depending on chosen parameters can be analyzed. A numerical realization is used to demonstrate the approach. The poles and the reflection zeros of a metasurface and their sensitivities with respect to geometrical parameters are computed. Furthermore, a modal expansion in the complex frequency plane is introduced to investigate the appearance of the reflection zeros through the interference of modal contributions.

*Singularities and contour integration.*—In the steady-state regime, light scattering in a material system can be described by the time-harmonic Maxwell's equation in second-order form,

$$\nabla \times \mu^{-1} \nabla \times \mathbf{E} - \omega_0^2 \epsilon \mathbf{E} = i\omega_0 \mathbf{J}, \quad (1)$$

where  $\mathbf{E}(\mathbf{r}, \omega_0) \in \mathbb{C}^3$  is the electric field,  $\mathbf{J}(\mathbf{r}) \in \mathbb{C}^3$  is the electric current density describing a light source,  $\epsilon(\mathbf{r}, \omega_0)$  and  $\mu(\mathbf{r}, \omega_0)$  are the permittivity and permeability tensors, respectively,  $\mathbf{r} \in \mathbb{R}^3$  is the position, and  $\omega_0 \in \mathbb{R}$  is the angular frequency.

Electromagnetic quantities  $Q(\mathbf{E}(\mathbf{r}, \omega_0)) \in \mathbb{C}$ , such as reflection or transmission coefficients, are typically

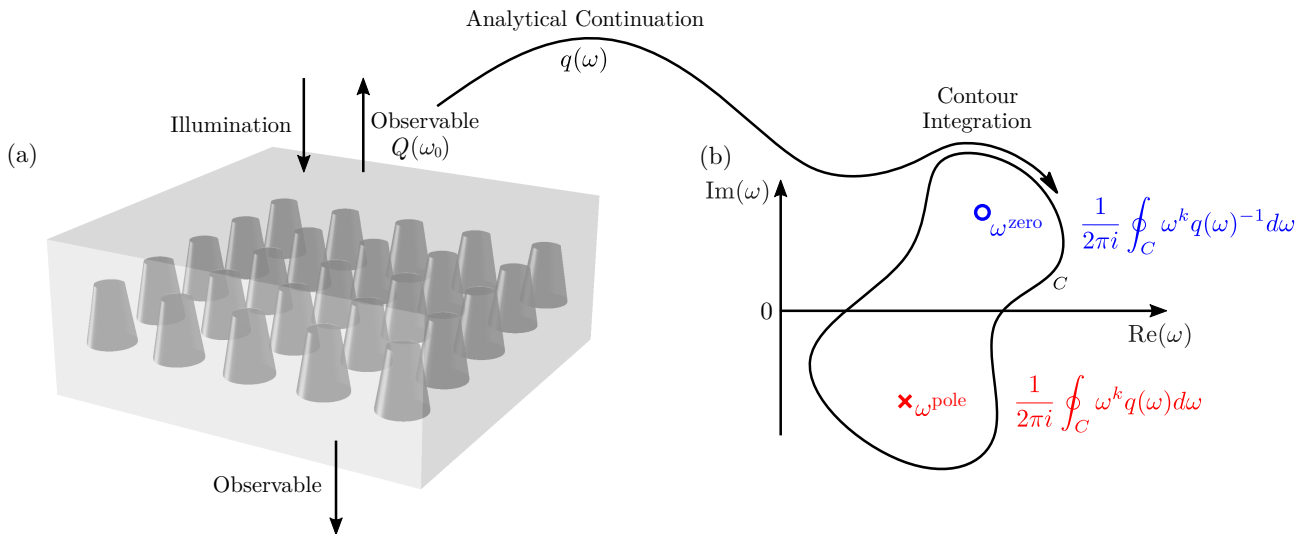


FIG. 1. Singularities of physical observables emerge in the complex frequency plane. (a) Schematic of a metasurface illuminated by a plane wave. The response of the nanostructure is typically described by resulting physical observables  $Q(\omega_0)$  for real excitation frequencies  $\omega_0 \in \mathbb{R}$ . The corresponding analytical continuation  $q(\omega)$  into the complex frequency plane  $\omega \in \mathbb{C}$  is considered. (b) Both quantities,  $q(\omega)$  and  $q(\omega)^{-1}$ , exhibit singularities in the complex frequency plane. A singularity of  $q(\omega)$  is denoted by  $\omega^{\text{pole}}$  and a singularity of  $q(\omega)^{-1}$  is denoted by  $\omega^{\text{zero}}$ . There exists a relation between contour integrals involving  $q(\omega)$  and  $q(\omega)^{-1}$ , respectively, and their singularities. This allows for determining the locations of  $\omega^{\text{pole}}$  and  $\omega^{\text{zero}}$ .

experimentally measured for real excitation frequencies  $\omega_0 \in \mathbb{R}$ . However, to obtain deeper insights into light-matter interactions, an investigation of the optical response for complex frequencies  $\omega \in \mathbb{C}$  is essential. For this, we consider the analytical continuation of  $Q(\mathbf{E}(\mathbf{r}, \omega_0))$  into the complex frequency plane, which we denote by  $q(\omega) \in \mathbb{C}$  as a short notation of  $q(\mathbf{E}(\mathbf{r}, \omega))$ . Figure 1(a) shows an example from the field of nanophotonics, a dielectric metasurface [22]. Illumination of the metasurface by a plane wave with the optical frequency  $\omega_0$  yields a physical observable  $Q(\omega_0)$ . The singularities of its analytical continuation  $q(\omega)$  and the singularities of  $q(\omega)^{-1}$  are of special interest and can be used to investigate the properties of the metasurface.

The singularities of  $q(\omega)$  are the poles  $\omega^{\text{pole}}$  of the physical quantity  $q(\omega)$ . The associated electric fields are so-called resonances or quasinormal modes. The singularities of  $q(\omega)^{-1}$  are the zeros  $\omega^{\text{zero}}$  of  $q(\omega)$ . The associated electric fields leads to  $q(\omega^{\text{zero}}) = 0$ . Figure 1(b) sketches the complex frequency plane with exemplary locations of a pole and a zero. By using Cauchy's integral theorem for a contour  $C$  which encloses one simple pole  $\omega^{\text{pole}}$  and (or) one simple zero  $\omega^{\text{zero}}$  of the quantity  $q(\omega)$ , as sketched in Fig. 1(b),  $\omega^{\text{pole}}$  and  $\omega^{\text{zero}}$  are given by

$$\omega^{\text{pole}} = \frac{\oint_C \omega q(\omega) d\omega}{\oint_C q(\omega) d\omega} \quad \text{and} \quad \omega^{\text{zero}} = \frac{\oint_C \omega q(\omega)^{-1} d\omega}{\oint_C q(\omega)^{-1} d\omega},$$

respectively. The locations of  $M$  poles  $\omega_m^{\text{pole}}$  inside a contour  $C$  are given by the eigenvalues  $\omega_m$  of the generalized

eigenproblem [23]

$$H^< X = H X \Omega, \quad (2)$$

where  $\Omega = \text{diag}(\omega_1, \dots, \omega_M)$  is a diagonal matrix containing the eigenvalues, the columns of the matrix  $X \in \mathbb{C}^{M \times M}$  are the eigenvectors, and

$$H = \begin{bmatrix} s_0 & \dots & s_{M-1} \\ \vdots & & \vdots \\ s_{M-1} & \dots & s_{2M-2} \end{bmatrix}, \quad H^< = \begin{bmatrix} s_1 & \dots & s_M \\ \vdots & & \vdots \\ s_M & \dots & s_{2M-1} \end{bmatrix}$$

are Hankel matrices with the contour-integral-based coefficients

$$s_k = \frac{1}{2\pi i} \oint_C \omega^k q(\omega) d\omega.$$

The zeros  $\omega_m^{\text{zero}}$  inside the contour are also given in this way, except that the quantity  $q(\omega)^{-1}$  is considered for the coefficients instead of  $q(\omega)$ . Note that this type of approach has inspired a family of numerical methods to reliably evaluate all zeros and poles in a given bounded domain. The methods are an active area of research in numerical mathematics, where, e.g., numerical stability, error bounds, and adaptive subdivision schemes are investigated [23–26].

To compute poles and zeros, the coefficients of the Hankel matrices can be approximated by numerical integration [27], where the quantity of interest  $q(\omega)$  is calculated by computing  $\mathbf{E}(\mathbf{r}, \omega)$  for complex frequencies on the integration contour  $C$ . The electric field  $\mathbf{E}(\mathbf{r}, \omega)$  can

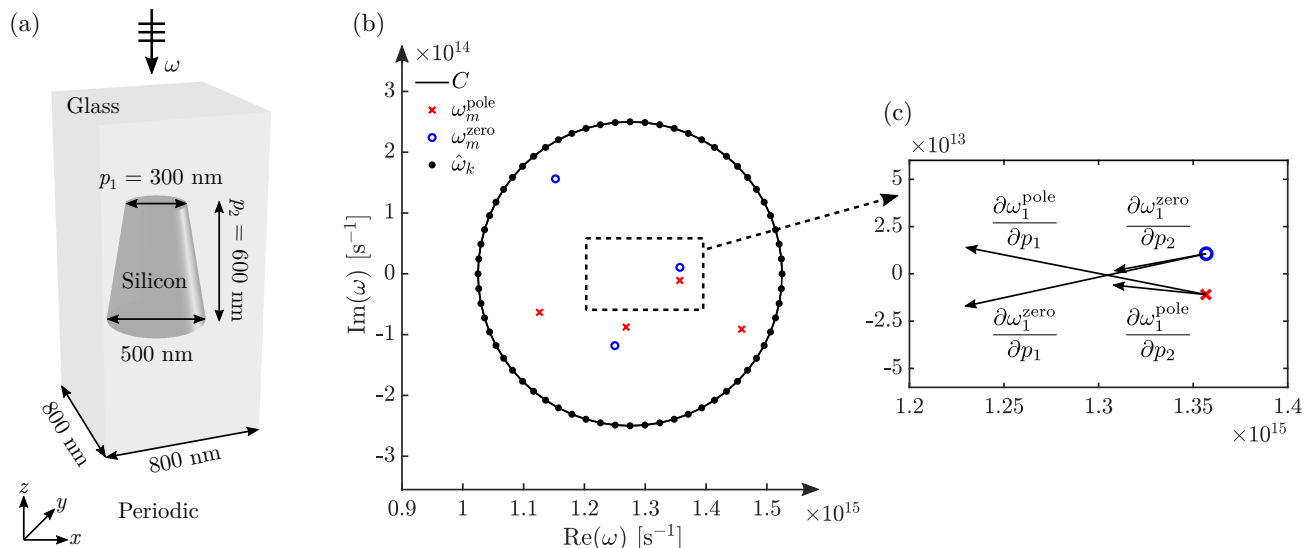


FIG. 2. Poles, reflection zeros, and their sensitivities of an illuminated metasurface. (a) Sketch of the periodic unit cell. The metasurface consists of silicon cones with upper radius  $p_1$  and height  $p_2$  embedded in glass. The refractive indices of silicon and glass are  $n = 3.5$  and  $n = 1.5$ , respectively. The illumination is given by a  $x$ -polarized plane wave of the optical frequency  $\omega$  at normal incidence from above. (b) Integration contour  $C$ , which is a circle with center  $1.275 \times 10^{15} \text{ s}^{-1}$  and radius  $2.5 \times 10^{14} \text{ s}^{-1}$ . The integration contour is numerically discretized by a trapezoidal rule with 64 integration points  $\hat{\omega}_k$  marked with black dots. The resulting poles  $\omega_m^{\text{pole}}$  and reflection zeros  $\omega_m^{\text{zero}}$  correspond to the Fourier coefficient  $q(\omega)$ . (c) Detail of the complex frequency plane comprising the two singularities  $\omega_1^{\text{pole}}$  and  $\omega_1^{\text{zero}}$ . The arrows are associated to the corresponding sensitivities  $\partial\omega_1^{\text{pole}}/\partial p_k$  and  $\partial\omega_1^{\text{zero}}/\partial p_k$  with respect to the shape parameters  $p_1$  and  $p_2$ . The sensitivities are also determined by integrals along the contour  $C$ . The complex-valued arrows are given by  $\delta\omega = \partial\omega/\partial p \times 100\text{nm}$ .

be obtained by numerically solving Maxwell's equation given in Eq. (1). The quantity  $q(\omega)^{-1}$  is immediately available by inverting the scalar quantity  $q(\omega)$ . Computing the different contour integrals for each of the coefficients requires no additional computational effort since the quantity  $q(\omega)$  needs to be calculated only once for each of the integration points. The integrands differ only in the weight functions  $\omega^k$ . Information on the numerical realization can be found in Ref. [28]. Further, the data publication [29] contains software for reproducing the results of this work based on an interface to the finite-element-based Maxwell solver JCMsuite.

*Poles and reflection zeros of a metasurface.*—We apply this approach to determine the poles  $\omega_m^{\text{pole}}$  and reflection zeros  $\omega_m^{\text{zero}}$  of the metasurface sketched in Fig. 1(a). Figure 2(a) shows the geometry of the nanostructures forming the metasurface, including the parameters chosen for the numerical simulation. The metasurface is illuminated by a plane wave at normal incidence from above. For the investigation of the reflected electric field, we consider the Fourier transform of  $\mathbf{E}(\mathbf{r}, \omega_0)$  [30]. Due to sub-wavelength periodicity, the resulting upward propagating Fourier spectrum consists of only one term, the zero-order diffraction coefficient  $Q(\omega_0)$ . Solving the generalized eigenproblem given by Eq. (2) with the analytical continuation  $q(\omega)$  of  $Q(\omega_0)$  gives the poles  $\omega_m^{\text{pole}}$  and the reflection zeros  $\omega_m^{\text{zero}}$  of the illuminated metasurface. We

$u$	$\text{Re}(u)$	$\text{Im}(u)$	$\text{err}(\text{Re}(u))$	$\text{err}(\text{Im}(u))$
$\omega_1^{\text{pole}}$	$1.357 \times 10^{15}$	$-1.095 \times 10^{13}$	$< 10^{-8}$	$3 \times 10^{-8}$
$\frac{\partial\omega_1^{\text{pole}}}{\partial p_1}$	$-1.257 \times 10^{12}$	$2.47 \times 10^{11}$	$8 \times 10^{-5}$	$6 \times 10^{-4}$
$\frac{\partial\omega_1^{\text{pole}}}{\partial p_2}$	$-4.782 \times 10^{11}$	$4.9 \times 10^{10}$	$7 \times 10^{-5}$	$2 \times 10^{-3}$
$\omega_1^{\text{zero}}$	$1.357 \times 10^{15}$	$1.066 \times 10^{13}$	$< 10^{-8}$	$3 \times 10^{-8}$
$\frac{\partial\omega_1^{\text{zero}}}{\partial p_1}$	$-1.26 \times 10^{12}$	$-2.8 \times 10^{11}$	$7 \times 10^{-4}$	$3 \times 10^{-3}$
$\frac{\partial\omega_1^{\text{zero}}}{\partial p_2}$	$-4.7 \times 10^{11}$	$8.8 \times 10^{10}$	$2 \times 10^{-3}$	$2 \times 10^{-3}$

TABLE I. Computed pole  $\omega_1^{\text{pole}}$  and zero  $\omega_1^{\text{zero}}$  in  $\text{s}^{-1}$  and their sensitivities  $\partial\omega_1^{\text{pole}}/\partial p_k$  and  $\partial\omega_1^{\text{zero}}/\partial p_k$  in  $(\text{s nm})^{-1}$ . The sensitivities are computed at the parameter reference values shown in Fig. 2(a) using the 64 integration points on the contour  $C$  depicted in Fig. 2(b). The relative error is defined by  $\text{err}(\text{Re}(u)) = |(\text{Re}(u) - \text{Re}(u_{\text{ref}}))/\text{Re}(u_{\text{ref}})|$ , where  $u_{\text{ref}}$  is the reference solution computed with 256 integration points.

emphasize that Eq. (2) provides an expression of both, poles and reflection zeros, and that the numerical implementation does not pose any difficulties. Figure 2(b) shows the integration contour  $C$  and the computed poles and zeros.

The contour-integral-based coefficients of the Hankel matrices in Eq. (2) allow to apply the approach of di-

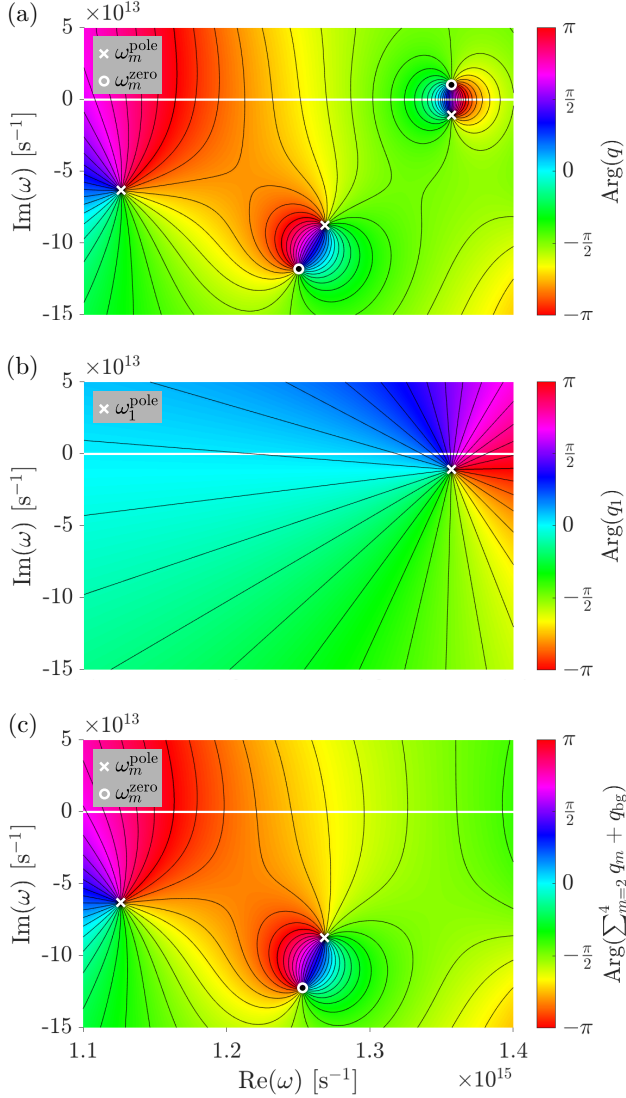


FIG. 3. Phase distribution of the electric field reflected from an illuminated metasurface and corresponding modal contributions. (a) Phase  $\text{Arg}(q(\omega))$  of the Fourier coefficient  $q(\omega)$  in a region enclosed by the contour  $C$  shown in Fig. 2(b). This phase distribution is obtained by a modal expansion where  $q(\omega)$  is computed only at the integration points  $\hat{\omega}_k$  on the contour  $C$ . As expected, the locations of the poles  $\omega_m^{\text{pole}}$  and zeros  $\omega_m^{\text{zero}}$  from Fig. 2(b), which are marked with white crosses and circles, respectively, coincide with the poles and zeros of the modal expansion  $\text{Arg}(q(\omega))$ . (b) Modal contribution  $\text{Arg}(q_1(\omega))$  to the phase. (c) Sum over remaining phase contributions,  $\text{Arg}(\sum_{m=2}^4 q_m(\omega) + q_{\text{bg}}(\omega))$ .

rect differentiation [31]. When the Fourier coefficients  $q(\hat{\omega}_k)$  are calculated at the integration points  $\hat{\omega}_k$  on the contour  $C$ , also their sensitivities  $\partial q/\partial p$  with respect to geometry, material, or source parameters  $p$  can be evaluated without significant additional computational effort. The sensitivities of the zeros can be extracted

in the same way as the sensitivities of the poles can be extracted [31]. Figure 2(c) sketches the sensitivities  $\partial\omega_1^{\text{pole}}/\partial p_k$  and  $\partial\omega_1^{\text{zero}}/\partial p_k$  with respect to the upper radius  $p_1$  and the height  $p_2$  of the silicon cones of the metasurface. With 64 integration points, it is possible to compute poles, zeros and their sensitivities with high accuracies, see Table I.

*Modal expansion in the complex frequency plane.*—The residues

$$a_m = \frac{1}{2\pi i} \oint_{C_m} q(\omega) d\omega,$$

where  $C_m$  are contours enclosing the single eigenvalues  $\omega_m$  from Eq. (2), can be used as a selection criterion for meaningful eigenvalues  $\omega_m$ . Eigenvalues with large  $a_m$  are prioritized, while  $\omega_m$  with small  $a_m$  are likely to be unphysical eigenvalues because either  $M$  is chosen larger than the actual number of eigenvalues within the contour or they are not significant with respect to the quantity of interest. Correspondingly, the choice of a specific source in Eq. (1) allows to regard only a subset of eigenvalues of the considered physical system [28, 29]. Note that, for simple eigenvalues, the residues are directly available, given by  $\text{diag}(a_1, \dots, a_M) = X^T H X$ , where  $X$  is suitably scaled [29].

Moreover, with the poles  $\omega_m^{\text{pole}}$  and the corresponding residues  $a_m$ , the modal expansion of the Fourier coefficient,

$$q(\omega) = \sum_{m=1}^M q_m(\omega) + q_{\text{bg}}(\omega), \quad (3)$$

$$q_m(\omega) = \frac{-a_m}{\omega_m^{\text{pole}} - \omega}, \quad q_{\text{bg}}(\omega) = \frac{1}{2\pi i} \oint_C \frac{q(\xi)}{\xi - \omega} d\xi,$$

can be performed, where  $q_m(\omega)$  are Riesz-projection-based modal contributions and  $q_{\text{bg}}(\omega)$  is the background contribution [32].

Figure 3(a) shows the phase distribution  $\text{Arg}(q(\omega))$  of the electric field reflected from the metasurface shown in Fig. 2(a). This is obtained by evaluating the modal expansion given by Eq. (3) for the contour  $C$  shown in Fig. 2(b). A phase retardation of  $2\pi$  for a real frequency scan, which is often required for the design of metasurfaces, is obtained when a pair of pole  $\omega_m^{\text{pole}}$  and zero  $\omega_m^{\text{zero}}$  is separated by the real axis [13]. Figure 3(b) shows  $\text{Arg}(q_1(\omega))$  corresponding to the pole  $\omega_1^{\text{pole}}$  and Fig. 3(c) shows  $\text{Arg}(\sum_{m=2}^4 q_m(\omega) + q_{\text{bg}}(\omega))$ . In particular, it can be observed that the zero  $\omega_1^{\text{zero}}$  does not appear for the modal contribution  $q_1(\omega)$ , but it emerges due to interference with the other contributions, i.e., when  $\sum_{m=2}^4 q_m(\omega) + q_{\text{bg}}(\omega)$  is added to  $q_1(\omega)$ .

*Conclusion.*—We presented a theoretical formulation to determine the locations of complex-valued singularities, including poles and zeros, of any electromagnetic quantity in photonic systems. The zeros can be determined by contour integration, in the same way as

the poles corresponding to resonances can be computed. We also presented modal expansions in the complex frequency plane of the phase of the field reflected from a metasurface, where the total expansion validated the computed reflection zeros. The different modal contributions give insight into the emergence of the reflection zeros by interference of various expansion terms. Furthermore, computation of partial derivatives of the reflection zeros was demonstrated. The approach can easily be transferred to other physical systems supporting resonances, e.g., to quantum mechanics and acoustics.

The theory essentially relies on detecting singularities of meromorphic functions in the complex plane. Therefore, it can be easily extended to compute other quantities, e.g., transmission zeros, scattering cross sections of isolated particles, or maximal chiral response of nanoassemblies. The real-frequency response of metasurfaces can in many cases be significantly impacted by reflection and transmission zeros, since these typically lie close to the real axis or can even cross the real axis with slight parameter variations. Therefore, a precise quantification of the sensitivities of reflection and transmission zeros or also of other physical quantities is essential for gradient-based optimization of photonic metasurfaces or other resonant or non-resonant systems. We expect that the presented theory will enable new computer-aided design approaches.

Supplementary data tables and source code for the numerical experiments for this work can be found in the open access data publication [29].

We acknowledge funding by the Deutsche Forschungsgemeinschaft (DFG, German Research Foundation) under Germany's Excellence Strategy - The Berlin Mathematics Research Center MATH+ (EXC-2046/1, project ID: 390685689), by the German Federal Ministry of Education and Research (BMBF Forschungscampus MODAL, project 05M20ZBM), and by the European Innovation Council (EIC) project TwistedNano (grant agreement number Pathfinder Open 2021-101046424).

- 
- [1] J. M. Raimond, M. Brune, and S. Haroche, *Rev. Mod. Phys.* **73**, 565 (2001).
- [2] S. Nie and S. R. Emory, *Science* **275**, 1102 (1997).
- [3] P. Senellart, G. Solomon, and A. White, *Nat. Nanotechnol.* **12**, 1026 (2017).
- [4] P. Lalanne, W. Yan, K. Vynck, C. Sauvan, and J.-P. Hugonin, *Laser Photonics Rev.* **12**, 1700113 (2018).
- [5] S. Dyatlov and M. Zworski, *Mathematical theory of scattering resonances* (American Mathematical Society, Providence, Rhode Island, 2019).
- [6] T. Wu, M. Gurioli, and P. Lalanne, *ACS Photonics* **8**, 1522 (2021).
- [7] C. Sauvan, T. Wu, R. Zarouf, E. A. Muljarov, and P. Lalanne, *Opt. Express* **30**, 6846 (2022).
- [8] A. Nicolet, G. Demésy, F. Zolla, C. Campos, J. E. Roman, and C. Geuzaine, *Eur. J. Mech. A Solids* **100**, 104809 (2023).
- [9] C. Desoer and J. Schulman, *IEEE Trans. Circuits Syst.* **21**, 3 (1974).
- [10] A. Oppenheim and G. Verghese, *Signals, Systems and Inference, Global Edition* (Pearson, 2017).
- [11] S. Butterworth *et al.*, *Wirel. Eng.* **7**, 536 (1930).
- [12] J. Bechhoefer, *Am. J. Phys.* **79**, 1053 (2011).
- [13] R. Colom, E. Mikheeva, K. Achouri, J. Zuniga-Perez, N. Bonod, O. J. F. Martin, S. Burger, and P. Genevet, *Laser Photonics Rev.* **17**, 2200976 (2023).
- [14] M. Hutley and D. Maystre, *Opt. Commun.* **19**, 431 (1976).
- [15] Y. D. Chong, L. Ge, H. Cao, and A. D. Stone, *Phys. Rev. Lett.* **105**, 053901 (2010).
- [16] D. Maystre, *C. R. Phys.* **14**, 381 (2013).
- [17] K. V. Sreekanth, S. Sreejith, S. Han, A. Mishra, X. Chen, H. Sun, C. T. Lim, and R. Singh, *Nat. Commun.* **9**, 369 (2018).
- [18] V. G. Kravets, A. V. Kabashin, W. L. Barnes, and A. N. Grigorenko, *Chem. Rev.* **118**, 5912 (2018).
- [19] V. Grigoriev, A. Tahri, S. Varault, B. Rolly, B. Stout, J. Wenger, and N. Bonod, *Phys. Rev. A* **88**, 011803(R) (2013).
- [20] A.-S. Bonnet-Ben Dhia, L. Chesnel, and V. Pagneux, *Proc. R. Soc. A* **474**, 20180050 (2018).
- [21] W. R. Sweeney, C. W. Hsu, and A. D. Stone, *Phys. Rev. A* **102**, 063511 (2020).
- [22] E. Mikheeva, R. Colom, K. Achouri, A. Overvig, F. Binkowski, J.-Y. Duboz, S. Cuffeff, S. Fan, S. Burger, A. Alu, and P. Genevet, *Optica Open. Preprint.* (2023), 10.1364/opticaopen.22828976.v1.
- [23] A. P. Austin, P. Kravanja, and L. N. Trefethen, *SIAM J. Numer. Anal.* **52**, 1795 (2014).
- [24] L. M. Delves and J. N. Lyness, *Math. Comp.* **21**, 543 (1967).
- [25] P. Kravanja and M. V. Barel, *Computing the Zeros of Analytic Functions, Lect. Notes Math. 1727* (Springer, New York, 2000).
- [26] H. Chen, *J. Comput. Appl. Math.* **402**, 113796 (2022).
- [27] L. N. Trefethen and J. Weideman, *SIAM Rev.* **56**, 385 (2014).
- [28] F. Betz, F. Binkowski, and S. Burger, *SoftwareX* **15**, 100763 (2021).
- [29] F. Binkowski, F. Betz, R. Colom, P. Genevet, and S. Burger, "Source code and simulation results: Poles and zeros of electromagnetic quantities in photonic systems," Zenodo (2023), doi: 10.5281/zenodo.8063932.
- [30] L. Novotny and B. Hecht, *Principles of Nano-Optics, 2nd ed.* (Cambridge University Press, Cambridge, 2012).
- [31] F. Binkowski, F. Betz, M. Hammerschmidt, P.-I. Schneider, L. Zschiedrich, and S. Burger, *Commun. Phys.* **5**, 202 (2022).
- [32] L. Zschiedrich, F. Binkowski, N. Nikolay, O. Benson, G. Kewes, and S. Burger, *Phys. Rev. A* **98**, 043806 (2018).